

Search for spin-slip lockins using tailored impurity layers

M. J. Conover* and C. P. Flynn

Department of Physics, University of Illinois at Urbana-Champaign, Urbana, Illinois 61801

Assunta Vigliante and Doon Gibbs

Department of Physics, Brookhaven National Laboratory, Upton, New York 11973

(Received 25 August 1997)

We have searched for spin-slip lockins with impurity layers introduced into Ho and Er as artificial superlattice perturbations. The locking interaction with the impurities appears to be weak or nonexistent. [S0163-1829(98)51402-6]

The helimagnetism exhibited by the $4f$ cores in rare-earth (RE) metals is a rich topic covering decades of research.¹⁻³ When the period of the magnetic order and the lattice spacing are mutually commensurate, these magnetic structures are believed to arise from fully periodic sequences of spin orientations in which an oscillatory basic pattern stabilized by strong crystal field anisotropy is modified by a periodic array of ‘‘spin slips.’’⁴⁻⁶ Spin slips are phase changes that break the basic oscillatory behavior. The much more common case of *incommensurate* order is described by an array of spin slips that is, to the contrary, *disordered*. The spin slip spacing arises from the interaction of the lattice spacing with the magnetic period τ_m . It is observed that the wavelength in incommensurate regions varies smoothly with temperature, upon which lockins at commensurate states appear as discrete regions with fixed wavelength.^{7,8} As they comprise magnetic anomalies that break the basic oscillation, spin slips also cause magnetoelastic modulation and so shift the ionic positions. In undertaking the present research, it has been our expectation that both the magnetic and positional changes introduced by spin slips can cause them to lock onto other periodicities of magnetism and strain inserted artificially into the lattice for just this purpose. We conceive that periodic arrays of magnetic and size defects introduced into the lattice during growth as magnetic impurities can thus provide a way to explore the interactions of spin slips with mechanical and magnetic structures. The effects are to be sought as new lockins at magnetic or ionic periodicities that reveal spin slips trapped at impurity planes. In fact, the central result of the present work is that the expected interactions are at best weak and at worst entirely beyond detection. The origins of this unexpected result are discussed.

In this paper we report experimental results for Er and Ho. These are hcp metals which exhibit paramagnetism above a Néel temperature T_N , ferromagnetism below a Curie temperature T_C , and, between T_N and T_C , helimagnetism (for Ho) or c -axis modulation (for Er) with oscillations propagating along the c axis. In Er the moments lie along c with a basic oscillation of four spins up followed by four down; spin slips comprise omitted spins as in the commensurate $2/7$ ferrimagnetic state which has four up then *three* down repeated, one slip each seven layers. As there exists a magnetic and a lattice anomaly every seven layers, one might try to lock these to an added perturbation from impu-

rity planes roughly each seven layers, and so explore the physics of the spin-slip interaction with the impurities by varying the impurity concentration and type. In Ho and Dy the spins align instead in the basal plane, along \mathbf{b} and \mathbf{a} in the respective cases. For Ho, the idealized helimagnetism has a 12 layer period with two layers in each of the six successive b directions; the base period is also 12 layers for Dy, but the smaller basal plane anisotropy energy in Dy results in no observed lockin states to commensurate wave vectors. In Ho the basic period is adjusted by spin slips as described above, and the same possibility arises that spin slips can be trapped by planes of impurity dopants.

In the limit of weak impurity effects, the impurity plane concentration C can be imagined as a superposition $C_0 + C(z)$ of the average value and the remaining position dependence $C(z)$; modifications of helimagnetic wavelength may then be ascribed to the average doping (which changes the average lattice spacing or magnetization) or to the attractive spatial interactions through $C(z)$. As the interaction remains poorly understood it is advisable to investigate both signs of impurity perturbation. We visualize the attraction as creating an artificial lockin at the temperature where the spin-slip spacing of an incommensurate region crosses the selected spacing of the doped planes.

To pursue these ideas we have grown superlattices (SL's) of Er which are doped with impurity planes of Y or Lu, and SL's of Ho with planes of Dy. In the case of Er, the nonmagnetic Y and Lu dopant layers provide strain modulations of 1–2% with opposite signs, and also interrupt the magnetic sequence. For Ho superlattices, the Dy layers provide a smaller strain modulation ($\approx 0.1\%$) but have a different magnetization direction (the a axis) from those in Ho (b axis), and thereby comprise a magnetic anomaly. Resonant magnetic x-ray scattering at beamline X22C of the National Synchrotron Light Source (NSLS) was employed to follow the helimagnetic wavelengths as a function of temperature through regions where artificial lockins become possible. Note in general that the spin-slip period differs from the magnetic wavelength for both Ho and Er, and that given a doping periodicity incommensurate with the wavelength, it does not interfere with the possible observation of a lockin. Several orders of superlattice peaks are readily observable in our samples and are used to determine the SL period Λ .

TABLE I. List of superlattice and film samples used in this study. Lengths are measured in atomic layers (L).

Sample	SL period (L)	Dopant (L)	Lockin $\tau_m(c^*)$	Slip period (L)
Er/Lu SL	14	1	6/23, 2/7	23, 7
Er/Y SL	19	1/4	5/19	19
Er/Y SL	29	1	5/19, 2/7	19, 7
Er/Y SL	33	1/2	None	None
Ho film	None	None	0.191 \approx 4/21	7
Ho/Dy SL	16	1	0.178 \approx 7/39	13
Ho/Dy SL	8	1	0.172	29

The rare-earth samples were prepared by MBE using a well-established growth procedure. First, Ta [011] from an electron beam source was evaporated onto sapphire [11 $\bar{2}$ 0] at a substrate temperature of 900 °C. Then, the substrate temperature was reduced to 700 °C and a [0001] Y_xLu_{1-x} alloy layer was coevaporated from effusion cell sources. The Y concentration x of the alloy was adjusted to match the in-plane lattice parameter of the subsequent RE layer, in order to make the next [0001] RE (Er, Ho) layer largely strain-free. For Er and Ho, the values x in the Y_xLu_{1-x} alloys were chosen to be $x = 33$ at. % and 54 at. %, respectively. Rare-earth films and multilayers were then deposited from effusion cell sources with the substrate held at a temperature of 400 °C. Table I lists the various films and SL's used in this study.

X-ray diffraction studies at NSLS reveal a high structural quality of the films and SL's. The beamline (X22C) used in this study employs a Ge [111] double-crystal monochromator, a focusing primary x-ray mirror, and a second Ge [111] crystal used as an analyzer. Figure 1 shows a radial scan of a Ho film at an x-ray energy of 8075 eV. It includes reflections from Ho, the sapphire substrate and the Ta base layer, and smaller peaks from the 300 Å Y cap layer and the magnetic periodicities. The $\Delta 2\theta = 0.017^\circ$ full width at half maximum (FWHM) of the sapphire (11 $\bar{2}$ 0) reflection can be taken to measure the machine resolution used in this experiment. Radial widths $\Delta 2\theta$ of the (0002) fundamental SL peak

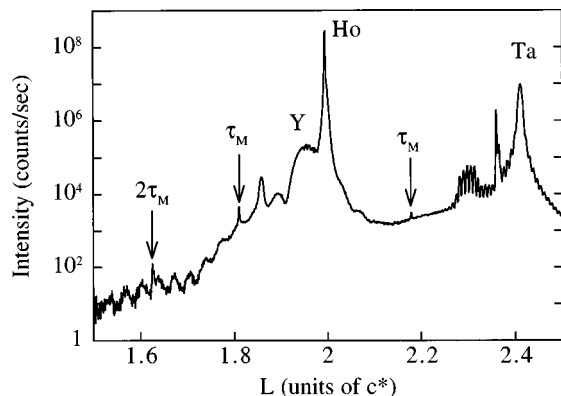


FIG. 1. [000 L] scan around Ho (0002) reflection for the 4000 Å Ho film. Peaks from the substrate, Ta base layer, Ho film, Y cap layer, and from magnetic x-ray scattering are labeled. Oscillations arising from interference between the front and back surfaces of the Ta layer and the Y cap layer can be seen near the Ta and Y Bragg peaks.

for Ho/Y and Er/Lu range from 0.02° to 0.03°. These widths correspond to calculated ΔQ on the order of 0.002 Å $^{-1}$ and calculated x-ray coherence lengths (2500–3500 Å) comparable to the 4000 Å thickness of these films. Coherence lengths were calculated using the Scherr formula, $L = 0.9 \lambda / (\cos \theta \Delta 2\theta)$, where L is the coherence length, λ is the x-ray wavelength, and $\Delta 2\theta$ is the FWHM of the radial peak in radians. The thinner Er/Y SL's (≈ 1200 Å) had much broader (0002) peaks of 0.1° to 0.2° FWHM, which reflect coherence lengths shorter than 1000 Å. Rocking curve widths of the (0002) reflection are on the order of 0.15° for Ho and Er/Lu and 0.3° for Er/Y. While the Ho/Dy and Er/Lu films clearly have better structural coherence, the Er/Y films had sufficient thickness and coherence for adequate measurement of the magnetic wave vector in this study.

Measurements of the magnetic wave vector employ the technique of resonant magnetic x-ray scattering. It has been shown for the heavy rare earths that magnetic scattering arises from polarization of the unoccupied 5d band by the magnetic moment of the core electrons and is detectable if the incident photons are tuned near the energy of the L_{III} edge.⁹ In this study, we excite the 2p-5d transition in Ho (8071 eV) and Er (8358 eV); these are dipole transitions which produce magnetically scattered photons with 90° polarization rotation relative to the incident beam. Polarization analysis was not attempted in this experiment. Instead, we identified magnetic peaks by their energy-resonant behavior and temperature dependence as compared to numerous published studies of similar RE films and superlattices. Values of τ_m were obtained from the diffractometer positions for the (0002), (0004), and magnetic peaks measured at each temperature. A standard procedure was used to find the reciprocal lattice spacing c^* and angular offset for each measurement and apply these to τ_m . The magnetic wave vector τ_m is plotted vs temperature T in Fig. 2(a) for Ho/Dy and Fig. 2(b) for Er/Y and Er/Lu.

In the Ho/Dy case, τ_m is shown for two SL samples with different periods and for a pure Ho film which serves as a reference. All curves of τ_m vs T vary smoothly with temperature and lock to a nearly constant wave vector below 20 K. The bulk lockin τ_m of 1/6 for Ho is not attained by any of these samples. Earlier work¹⁰ on Ho spin slips yielded the relationship of the slip wave vector, τ_s , to the magnetic wave vector as $\tau_s = 12\tau_m - 2$; the superlattice periods and calculated values of τ_m corresponding $\tau_s = \tau_{SL}$ are plotted in Fig. 2(a). We note that the low-temperature lockin for the (Ho 15/Dy 1) SL is very near to the predicted τ_m for the

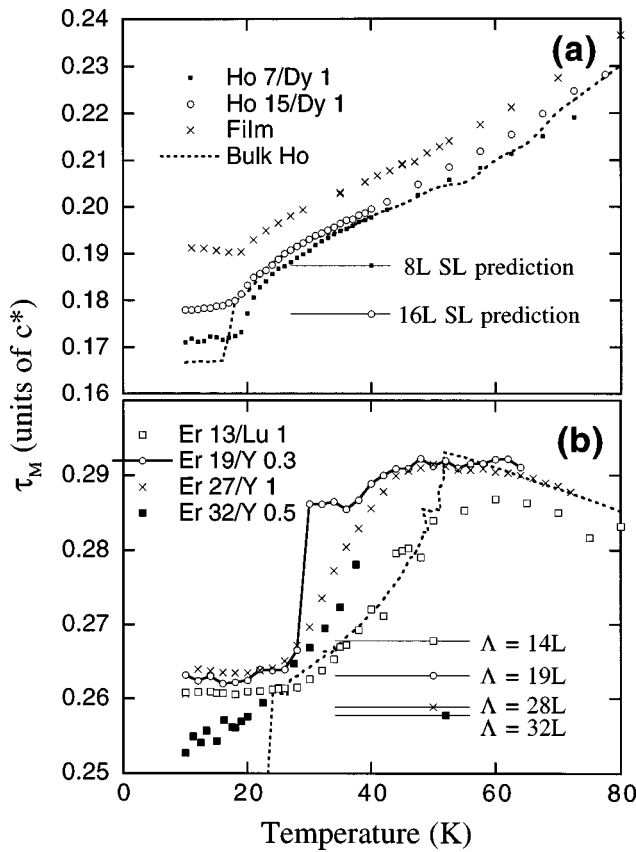


FIG. 2. (a) Magnetic wave vector for Ho film and two Ho/Dy superlattices. Predicted lockin τ_m for $\Lambda = 8$ layer and $\Lambda = 16$ layer superlattices are shown. Bulk Ho (Ref. 11) locks to a wave vector of $1/6$ (≈ 0.1667) at low temperatures. (b) Magnetic wave vector for the Er/Y superlattices, bulk Er, and the Er 13/Lu 1 SL. Predicted lockins for all SL's are shown by SL period Λ . Only the Er 19/Y 0.3 has a lockin to its predicted value. Bulk lockin data from Ref. 12 are shown by a dotted line.

built-in periodicity of that SL. However, the lockin of the (Ho 7/Dy 1) does not correspond at all to its predicted τ_m . In fact, it is shifted in the wrong sense (i.e., decreases) relative to that of the other SL. If the film and two SL samples are taken as a set, a general trend of decreasing lockin τ_m (τ_m approaching that of bulk Ho) occurs with increasing Dy concentration. Measurements of the c -axis lattice parameter over the same temperature range [Fig. 3(a)] show that an increased Dy concentration in the SL's indeed brings the lattice strain closer to that of bulk Ho.¹¹ We suggest that residual epitaxial strain, as measured by the c -axis length, may determine the low-temperature lockin τ_m . This associates the changes with C_0 rather than the spatially varying concentration $C(z)$.

If small *perturbations* of the τ_m variations with T are considered instead of *lockins*, then some evidence exists for an interaction between the SL period and τ_m . The two curves of τ_m for superlattices each display small irregularities near values of τ_m corresponding to an eight layer τ_s . Since both SL periods are multiples of eight layers, the irregularities in τ_m could thus correspond to a small interaction of the slip period to the superlattice period. However, the apparent τ_m perturbations are smaller than the estimated fitting uncertainties for the magnetic peaks, so the only

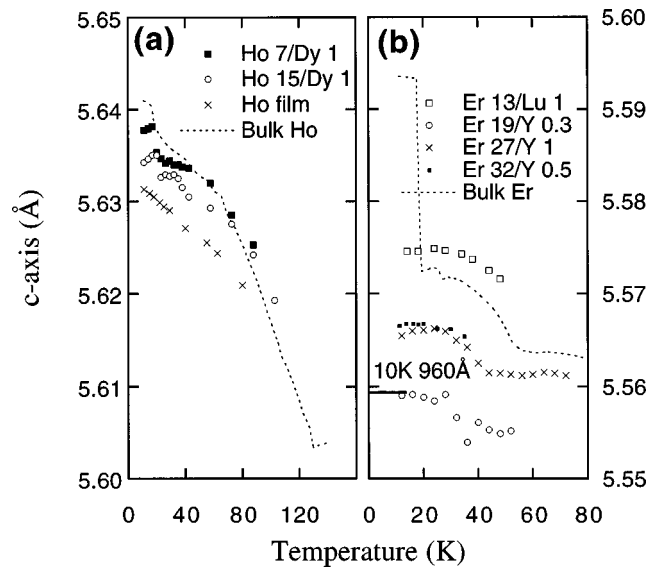


FIG. 3. (a) c -axis lattice parameter for Ho film, Ho 15/Dy 1 and Ho 7/Dy 1 SL's, and bulk Ho. Note that increasing Dy content is associated with more bulklike lattice spacings. Bulk data are from Ref. 11. (b) c -axis lattice spacing for bulk Er, Er 14/Lu 1 and the Er/Y SL's. Bulk data are from Ref. 11. The 10 K c -axis spacing for an 860 Å film (Ref. 14) is indicated by the solid line.

meaningful conclusion from the Ho/Dy SL's is that any interaction of the slip and SL periods is at the limits of detection. Given the high capabilities of the beamline this certainly establishes that the lockin energies sought here must be weak.

In the cases of Er/Y and Er/Lu we find similar results. Figure 2(b) compares the variation of τ_m with T for three Er/Y SL's and one Er/Lu SL with data for bulk Er measured in a previous study.¹² The relationship between τ_m and τ_s for Er is $\tau_s = 8\tau_m - 2$. A striking feature of Fig. 2(b) is the large difference in temperature dependence between the Er/Y samples and the bulk and Er/Lu samples. Although the Er 19/Y 0.25 SL apparently locks to $\tau_m = 5/19$, implying $\tau_s = \tau_{SL} = 2/19$, and to $2/7$ so that $\tau_s = 2/7$, none of the other samples show lockins with slip-wave vectors that are commensurate with either the fundamental or any multiple of the artificial SL periodicities. Note that *both* signs of strain modulation have been explored, since the lattice spacing of Y in the basal plane is 2.5% larger than that of Er while the spacing of Lu is 1.2% smaller. The lockin of the 19L Er/Y superlattice to $5/19$ might appear to indicate the sought interaction of spin slips with the superlattice. However, epitaxial strain is again a more likely cause for the apparent agreement between τ_s and the superlattice period. An earlier neutron diffraction study of an 860 Å film grown on an Y buffer layer showed the same lockins, $5/19$ and $2/7$, occurring at the same temperatures as for the Er 19/Y 0.25 SL.¹³ Furthermore, the c -axis lattice parameter of 5.557 Å measured for Er 19/Y 0.25 at 10 K is nearly the same as that of the 860 Å film (5.559 Å) found in the earlier study.¹⁴ Figure 3(b) compares the measured c -axis spacing for all samples in this study with bulk Er and with the strained film of Borchers *et al.* The Er 13/Lu film has a larger c -axis spacing than that of the bulk while the Er/Y films have a c -axis length smaller than bulk Er, and in rough proportion to the Y concentration.

As in the Ho/Dy case, the epitaxial strain measured by the c -axis spacing seems to determine the magnetic lockin behavior. Note that a layer of the larger atom, Y, expands the Er basal plane in order to maintain atomic registry, which in turn causes the Er c -axis to contract via Poisson's ratio. The opposite behavior, namely a basal plane contraction and c -axis expansion, is observed for Lu interlayers.

In summary, this search for the interaction of spin slips with SL doping has explored both periodic strain and magnetic perturbations. For Ho/Dy, the intervening Dy layers provide a potentially different magnetization direction and a modest strain perturbation. In the Er/Y(Lu) SL's, the non-magnetic Y(Lu) layers provide a large ($\approx 1-3\%$) strain perturbation and a nearly complete local removal of the Er magnetic moment from the Er magnetic structure. No strong lockin attributable to a spin-slip interaction with the SL period is found for any system investigated in this study, although perturbations in the τ_m vs temperature curves of the Ho/Dy SL's do suggest a small effect. Because an interaction of this type is expected, we conclude that its magnitude must be comparable with or below the detection limits of this experiment.

Numerous previous investigations of RE superlattices have concluded that periodic magnetic structures are coupled via indirect exchange across intervening Y or Lu layers.^{13,15-17} The measured τ_m for many of these films has been separated into a temperature-dependent turn angle in the RE and a temperature-independent turn angle of about $50^\circ/\text{layer}$ in the Y or Lu. None of these studies report incidental lockins of spin slips to the interfaces or to the superlattice periods, although no systematic effort has been made to find or eliminate this effect. The present study employs atomic structures specifically designed to explore this potential effect but fails to establish the existence of a locking interaction within the available detection limits. The results thus provide a challenge for theory to explain why the locking to artificial impurity perturbations appears so much weaker than certain clearly visible commensurate states at which the helimagnetism locks to the translationally invariant perfect lattice.

The University of Illinois portion of this project was supported by Grant No. NSF-DMR-94-24339. Work performed at BNL was supported by the U.S. DOE under Contract No. DE-AC02-76CH00016.

*Present address: Seagate Technology, 7801 Computer Ave. S., Bloomington, MN 55435.

¹R. J. Elliott, *Magnetic Properties of Rare Earth Metals* (Plenum, New York, 1972).

²B. Coqblin, *The Electronic Structure of Rare-Earth Metals and Alloys: The Magnetic Heavy Rare-Earths* (Academic, New York, 1977).

³Jens Jensen and Allan R. Mackintosh, *Rare Earth Magnetism* (Clarendon, Oxford, 1991).

⁴Jakob Bohr, Doon Gibbs, D. E. Moncton, and K. L. D'Amico, *Physica B & C* **140A**, 349 (1986).

⁵Per Bak and J. von Boehm, *Phys. Rev. B* **21**, 5297 (1980).

⁶W. L. McMillan, *Phys. Rev. B* **14**, 1496 (1976).

⁷W. C. Koehler, J. W. Cable, M. K. Wilkinson, and E. O. Wollan, *Phys. Rev.* **151**, 414 (1966).

⁸M. Habenschuss, C. Stassis, S. K. Sinha, H. W. Deckman, and F. H. Spedding, *Phys. Rev. B* **10**, 1020 (1974).

⁹M. Blume and Doon Gibbs, *Phys. Rev. B* **37**, 1779 (1988).

¹⁰Doon Gibbs, D. E. Moncton, K. L. D'Amico, J. Bohr, and B. H.

Grier, *Phys. Rev. Lett.* **55**, 234 (1985).

¹¹G. Helgesen, J. P. Hill, T. R. Thurston, and Doon Gibbs, *Phys. Rev. B* **52**, 9446 (1995).

¹²Doon Gibbs, Jakob Bohr, J. D. Axe, D. E. Moncton, and K. L. D'Amico, *Phys. Rev. B* **34**, 8182 (1986).

¹³J. A. Borchers, M. B. Salamon, R. W. Erwin, J. J. Rhyne, G. J. Nieuwenhuys, R. R. Du, C. P. Flynn, and R. S. Beach, *Phys. Rev. B* **44**, 11 814 (1991).

¹⁴J. A. Borchers, M. B. Salamon, R. W. Erwin, J. J. Rhyne, R. R. Du, and C. P. Flynn, *Phys. Rev. B* **43**, 3123 (1991).

¹⁵C. P. Flynn and M. B. Salamon, in *Handbook on the Physics and Chemistry of Rare Earths*, edited by Jr. Karl, A. Gschneidner, and LeRoy Eyring (Elsevier, Amsterdam, 1996), pp. 1-79.

¹⁶D. F. McMorrow, D. A. Jehan, P. P. Swaddling, R. A. Cowley, R. C. C. Ward, and M. R. Wells, *Physica B* **192**, 150 (1993).

¹⁷M. B. Salamon, Shantanu Sinha, J. J. Rhyne, J. E. Cunningham, Ross W. Erwin, Julie Borchers, and C. P. Flynn, *Phys. Rev. Lett.* **56**, 259 (1986).